Available online at www.sciencedirect.com

ScienceDirect

Ceramics International 42 (2016) 3096–3103

CERAMICS INTERNATIONAL

www.elsevier.com/locate/ceramint

Photocatalytic degradation of organic compounds by $PbMoO_4$ synthesized by a microwave-assisted solvothermal method

D.B. Hernández-Uresti[a,*], A. Martínez-de la Cruz[b], L.M. Torres-Martínez[c]

[a]*Universidad Autónoma de Nuevo León, CICFIM-Facultad de Ciencias Físico Matemáticas, Cd. Universitaria, C.P. 66455 San Nicolás de los Garza, N.L., México*
[b]*Universidad Autónoma de Nuevo León, CIIDIT-Facultad de Ingeniería Mecánica y Eléctrica, Cd. Universitaria, C.P. 66455 San Nicolás de los Garza, N.L., México*
[c]*Universidad Autónoma de Nuevo León, Facultad de Ingeniería Civil-Departamento de Ecomateriales y Energía, Cd. Universitaria, C.P. 66455 San Nicolás de los Garza, N.L., México*

Received 23 September 2015; received in revised form 19 October 2015; accepted 19 October 2015
Available online 24 October 2015

Abstract

The microwave-assisted solvothermal (PbMH) and conventional solvothermal (PbH) synthesis were successfully used to prepare $PbMoO_4$ particles with different morphologies, crystallinity degree and particle size. The material was structurally characterized by X-ray diffraction (XRD), their morphologies were investigated by scanning electron microscopy (SEM) and transmission electron microscopy (TEM). The textural and optical properties were analyzed by adsorption–desorption N_2 isotherms (BET), diffuse reflectance spectroscopy (DRS) and photoluminescence (PL) measurements, respectively. The photocatalytic activity of $PbMoO_4$ particles was evaluated by degradation of indigo carmine (IC), orange G (OG), tetracycline (TC), salicylic acid (SA) and ciprofloxacin (CIP) compounds in aqueous solution under UV–vis light irradiation. The PbMH sample showed the highest photocatalytic activity reaching half-life times ($t_{1/2}$) of 6, 7, 18, 75 and 125 min for TC, CIP, IC, SA and OG. Moreover, $PbMoO_4$ samples were evaluated in the H_2 production from aqueous solutions using ethanol as sacrificial agent. The results showed that the PbH sample has the highest photocatalytic activity for hydrogen generation probably attributed to its high crystallinity degree.

Keywords: $PbMoO_4$; Antibiotic degradation; Dye degradation; Hydrogen production

1. Introduction

A major environmental concern is the negative effect of wastewater pollution on both humans and the environment. Nowadays, the excessive use of antibiotics and its discharge into the environment cause negative effects on animals and human beings [1]. Conventional urban wastewater treatment plants can eliminate the organic matter, but the antibiotics pollutants are not oxidized. Ciprofloxacin (CIP) is a broad-spectrum antibacterial agent used in the bacterial infection [2], the tetracycline (TC) is considered as the antibiotic mostly used in veterinary medicine [3] and salicylic acid (SA) is produced by deacetylation of acetylsalicylate [4]. The three medicaments are often found in effluents, which have a negative impact on the environment and human health by the persistency and resistance of them.

Also, wastewater can contain different kind of dyes, which are mostly carcinogenic, toxic and persistent. Indigo carmine (IC) is widely used in textile industry and employed as additive in pharmaceutical capsules and tablets [5,6]. Orange G is an azo dye which has been extensively used by several industries [7,8].

In this respect, advanced oxidation processes (AOPs) such as heterogeneous photocatalysis [9–13] have shown great efficiency because the organic molecules causing the pollution can be eliminated from the treated wastewater. Heterogeneous photocatalysis is based on the generation in situ of powerful transitory species when a semiconductor absorbs visible or ultraviolet radiation to generate electron–hole pairs and

*Corresponding author. Tel.: +52 81 83 29 40 30.
E-mail address: ing.dianahdz@gmail.com (D.B. Hernández-Uresti).

http://dx.doi.org/10.1016/j.ceramint.2015.10.098
0272-8842/

produce hydroxyl radicals (●OH) for easily removing the pollutants from the wastewater by a total or partial mineralization of the organic carbon to CO_2 [14–18].

Moreover, the photocatalysis heterogeneous is also widely used to the generation of hydrogen from water using sunlight or other source irradiation, as renewable source of energy because of its simplicity [19–21]. The crystallinity and particle size are the main properties that affect the photocatalytic activity of a semiconductor for H_2 and O_2 evolution by water splitting [22–24]

The objective of this work is to establish if $PbMoO_4$ obtained by a microwave-assisted solvothermal method can be used to successfully remove tetracycline, ciprofloxacin, indigo carmine, orange G and salicylic acid from water and also for hydrogen production by splitting of water.

2. Experimental

2.1. Synthesis of $PbMoO_4$ powders

$PbMoO_4$ samples were prepared by the microwave-assisted solvothermal method (PbMH) in the presence of ethylene glycol (EG) and distilled water (DW). For this purpose, 5 mM of molybdic acid (H_2MoO_4) (85% purity, Sigma Aldrich) and 5 mM of lead nitrate [$Pb(NO_3)_2$] (99% purity, Sigma Aldrich) were dissolved in 35 mL of a mixture of 50% of EG and 50% of DW under vigorous stirring. The pH of the solution was adjusted to 11 by adding ammonium hydroxide (NH_4OH) (30%, JT. Baker). Afterwards, the resulting solution was sonicated for 30 min at room temperature, and posteriorly transferred into a microwave-assisted solvothermal dispositive and heated with a power of 200 W at 150 °C for 30 min. The resulting precipitate was washed with DW and ethanol several times to neutralize the pH of the solution and finally dried in air at 70 °C overnight.

In an alternate method, a second sample of $PbMoO_4$ powders was prepared by a conventional solvothermal method (PbH) from aqueous solutions of $Pb(NO_3)_2$ and H_2MoO_4 as it was described previously. The resulting solution was transferred into a 600 mL Teflon-lined stainless steel autoclave. Then, the autoclave was sealed and heated at 150 °C for 30 min. Finally, the autoclave was cooled down to room temperature. The precipitate formed was washed several times with DW and absolute alcohol, and dried at 70 °C for 12 h.

2.2. Characterization

$PbMoO_4$ samples were characterized by X-ray powder diffraction using a Bruker D8 advanced diffractometer with CuKα radiation ($\lambda = 1.5418$ Å) coupled with a Vantec high speed detector and Ni filters. X-ray diffraction data of the samples was collected in the 2θ range of 10–60 ° with a scan rate of 0.05° s^{-1}. The specific surface area was determined by N_2 adsorption–desorption isotherms by the Brunauer–Emmett–Teller (BET) method in a Bel-Japan Minisorp II Surface Area & Pore Size analyzer. The energy band gap value (E_g) of $PbMoO_4$ samples was determined from the UV–vis diffuse reflectance absorption spectrum of each sample by using a UV–vis–NIR spectrophotometer (Cary 5000) equipped with an integrating sphere. The morphology and particle size of the samples were investigated by scanning electron microscopy in a FEI Nova 200 Nano-SEM microscope operated at low vacuum and by transmission electron microscopy (TEM) in a JEOL 2010 microscope with an accelerating voltage of 200 kV. The recombination of the electron–hole pairs in $PbMoO_4$ was investigated by photoluminescence (PL) emission spectra, using an excitation light source of 350 nm. The emission from the sample was measured by a spectrometer Agilent Technologies Cary Eclipse Fluorescence Spectrophotometer.

2.3. Photocatalytic experiments

The photocatalytic activity of $PbMoO_4$ samples was evaluated by the degradation reaction under UV–vis light irradiation of different organic molecules, such as indigo carmine (30 mg L^{-1}) and orange G (20 mg L^{-1}) as dyes pollutants; and tetracycline (20 mg L^{-1}), salicylic acid (20 mg L^{-1}) and ciprofloxacin (10 mg L^{-1}) as pharmaceutical compounds. The photocatalytic reactions were performed in a borosilicate reactor (300 mL) equipped with a circulating cooling water system. A Xe lamp of 35 W (6,000 K) was used as source of simulated sunlight irradiation. In a typical reaction, the load of the photocatalyst was 1 g L^{-1}. The dispersion was sonicated and reposed in dark conditions during 1 h to ensure that the equilibrium adsorption–desorption of the organic compound on the catalyst surface was reached. After this time, the light source was turned on and several aliquots were taken from the reactor at different irradiation times. Then, the aliquots were analyzed following the procedures established in a previous work [4]. The mineralization degree was monitored by measuring the total organic carbon content (TOC) in the solutions at different time intervals. In the mineralization experiment, 250 mL of the corresponding solution (50 mg L^{-1} for OG, TC, SA and CIP; and 100 mg L^{-1} for IC) with 1 g L^{-1} as load of the photocatalyst was employed. The aliquots were analyzed in a Shimadzu VSCN8 TOC analyzer.

2.4. Water splitting experiments

Water splitting was carried out in a borosilicate reactor (250 mL) using a pen-ray lamp (UVP, 254 nm and 4400 μW cm^{-2}) as radiation source. First, 200 mg of the photocatalyst was dispersed in 200 mL of 80% deionized water and 20% ethanol under vigorous stirring. Afterwards, the solution was purged by bubbling nitrogen during 30 min and then the pen-ray lamp was turn on. The analysis of H_2 evolved was carried out in intervals of 30 min for 180 min using gas chromatography on an online Thermo Scientific gas chromatograph equipped with a thermal conductivity detector (TCD) and a fused silica capillary column (30 m × 0.53 mm).

3. Results and discussions

3.1. Characterization

XRD analysis of the different samples prepared by the microwave-assisted solvothermal (PbMH) and conventional solvothermal (PbH) method is shown in Fig. 1. All diffraction peaks were assigned with the tetragonal structure of $PbMoO_4$ with space group $I4_1/a$, which are in agreement with the reported data in the JCPDS Card no. 01-071-4910. The diffraction peaks indicate that the powders are well crystallized without any peaks assigned to either $Pb(NO_3)_2$, H_2MoO_4 or other phases. An enlarged view of the principal diffraction peak (112) of $PbMoO_4$ as is seen onset Fig. 1 shows that PbH oxide exhibited a higher intensity of the diffraction peak than the PbMH sample. Afterwards, the crystallite size and lattice strain were determined for the PbMH and PbH samples, as is shown in Table 1. The PbH sample has the highest crystallite size and the lowest lattice strain which evidencing the increment of the crystallinity in the $PbMoO_4$ sample obtained by the solvothermal method [25]. The Brunauer–Emmett–Teller method was used to determine the surface area, as is shown in Table 1. The optical properties of $PbMoO_4$ samples were analyzed by UV–vis diffuse reflectance spectroscopy. The energy band gap (E_g) values were calculated and listed in Table 1. Values of E_g of 3.16 eV (PbMH) and 3.21 eV (PbH) were calculated from the onset of the absorption edge for each data of $PbMoO_4$ samples. These data are in good agreement with the values reported in our previous works [26].

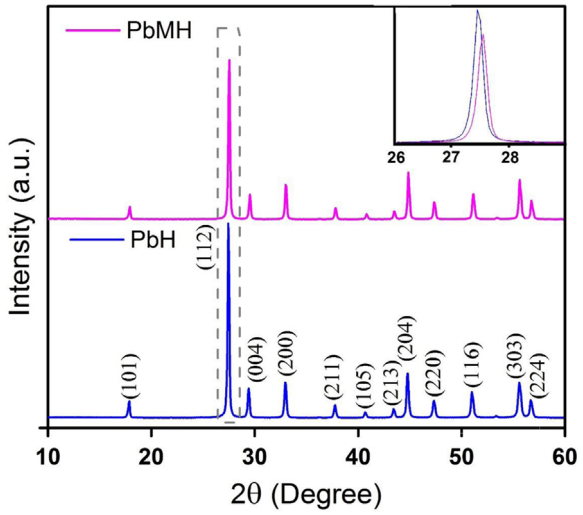

Fig. 1. XRD patterns of $PbMoO_4$ (a) synthesized by the microwave-assisted solvothermal and solvothermal method, and close up view (b) of the main diffraction peak in $PbMoO_4$ patterns.

The morphology and particle size of the $PbMoO_4$ samples were analyzed by SEM and formation of PbMH particles was also investigated. The sample prepared by the microwave-assisted solvothermal method is formed by aggregates with ovoid morphology and their sizes were around 80 nm, as seen in Fig. 2(a)–(b). On other hand, sphere-like particles with irregular shape and size around 1.1 μm were obtained by the solvothermal method, as is shown in Fig. 2(c)–(d). This is a very important point, because in contrast to what was observed for physical properties previously reported (crystallite size, lattice strain, specific surface area and E_g) it is noteworthy the difference on the morphology and size of the $PbMoO_4$ particles, indicating that microwave irradiation had a notably influence in these parameters. A possible formation mechanism of the $PbMoO_4$ nanoparticles obtained by the microwave-assisted solvothermal method is shown in Fig. 3(a). $PbMoO_4$ was produced when the lead and molybdate ions were dissolved in an alkaline solution in the microwave equipment. Afterwards the nucleation, the particles tend to form aggregates due to the Ostwald Ripening process, which could be the possible mechanism in the formation of the nanoparticles. The HRTEM images seem to confirm this hypothesis, as can be seen in Fig. 3(b)–(c) where is revealed many tiny nanoparticles (2–5 nm) located on the surface of the bigger nanoparticles.

3.2. Photocatalytic experiments

Commonly the organic compounds are degraded by UV radiation. Hence, it should be examined to what extent the pollutants are degraded in the absence of the photocatalyst. The degradation of pollutants by effect of photolysis was only up 12% for ciprofloxacin (CIP), 8% for tetracycline (TC) and 2% for the indigo carmine (IC), orange G (OG) and salicylic acid (SA). The photocatalytic experiments for IC degradation with $PbMoO_4$ catalyst under UV–vis light irradiation are presented in Fig. 4(a). After photocatalytic reaction for 60 min, the photocatalysts performed a total bleached of the IC solution, with a half-time of $t^1/_2 = 18$ and 35 min for PbMH and PbH, respectively. One key factor to increase the photocatalytic activity is the surface area. However, PbH and PbMH samples had no significant differences in the BET values. The enhanced photocatalytic activity can be attributed to the particle size causing a decrease in the way to follow the electron–hole pair from the point of its generation until the surface of the photocatalyst [27]. Photoluminescence (PL) spectroscopy was used to evaluate the recombination of the charges in the semiconductor particles. Fig. 5 shows the comparison of PL spectra of PbMH and PbH at 350 nm as wavelength excitation. As can be noted in the graphs, the PL

Table 1
Physical properties of $PbMoO_4$ synthesized by the microwave-assisted solvothermal and solvothermal method.

Sample	Crystalline size (nm)	Lattice strain (%)	Particle size	Surface area ($m^2\ g^{-1}$)	Band gap (eV)
PbH	110	0.241	1.1 m	1.95	3.21
PbMH	75	0.270	80 nm	2.06	3.16

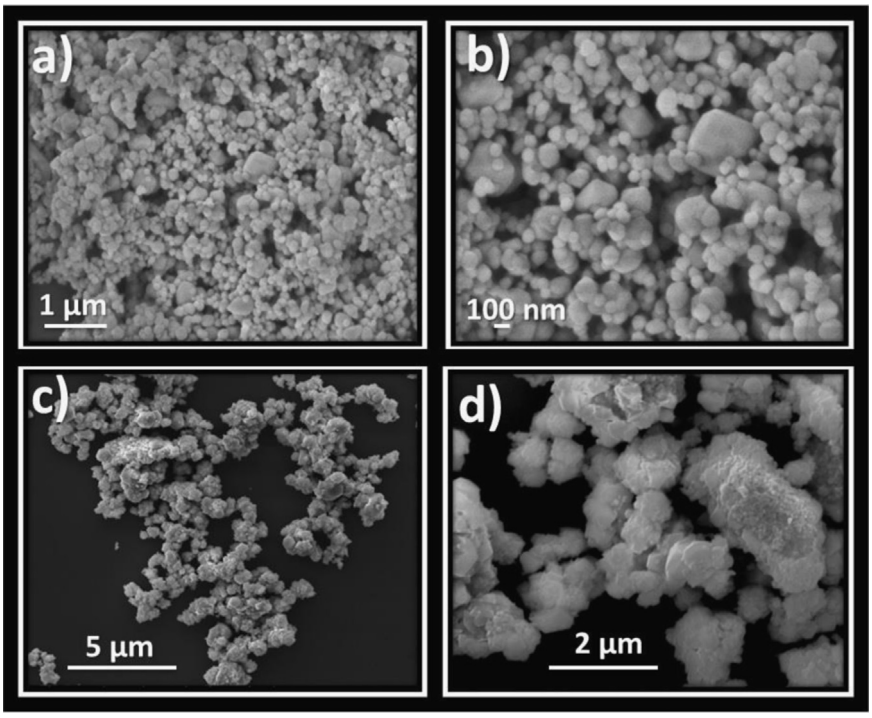

Fig. 2. SEM images of the morphology of $PbMoO_4$ synthesized by (a, b) the microwave-assisted-solvothermal method and (c, d) solvothermal reaction.

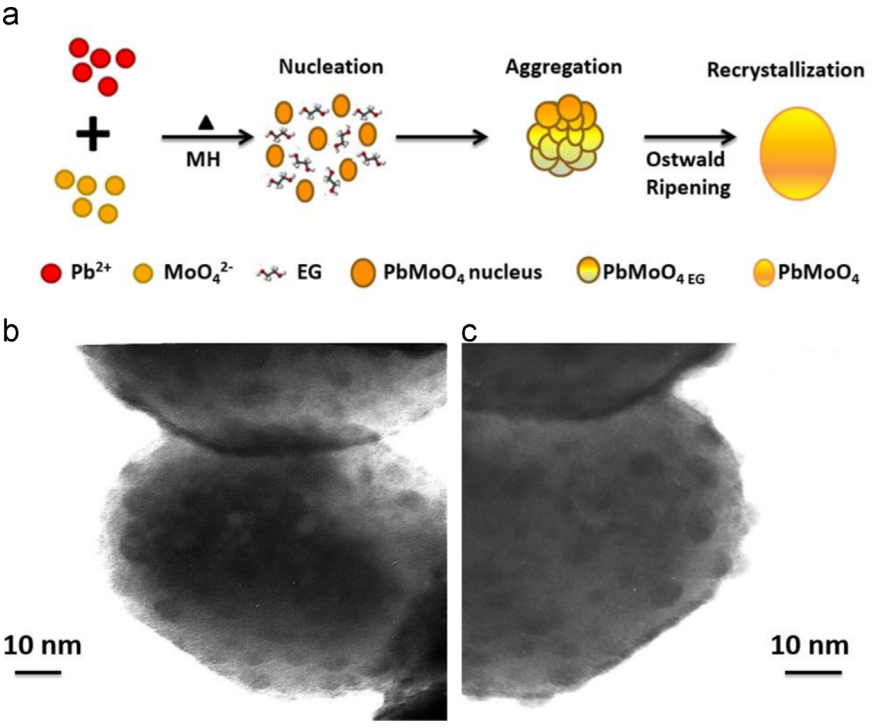

Fig. 3. Schematic diagram of the mechanism (a) and HRTEM images (b) of $PbMoO_4$ particles prepared by the microwave-assisted solvothermal method.

intensity lines of PbMH sample are lower than the lines of PbH, which implies that the recombination rate of electrons in orbitals was diminished under light irradiation. The PL as well as electrical properties depends on the morphology and particle size. A second organic dye was tested, in order to check the ability of $PbMoO_4$ samples to eliminate more recalcitrant molecules such as orange G. In Fig. 4(b), the photodegradation of OG was negligible under UV–vis light irradiation in the absence of the photocatalysts. However, the removal rate of OG was modified when introducing the PbH and PbMH samples. After 240 min of irradiation, about 65% of OG was removed in the presence of the PbMH sample. In contrast, only

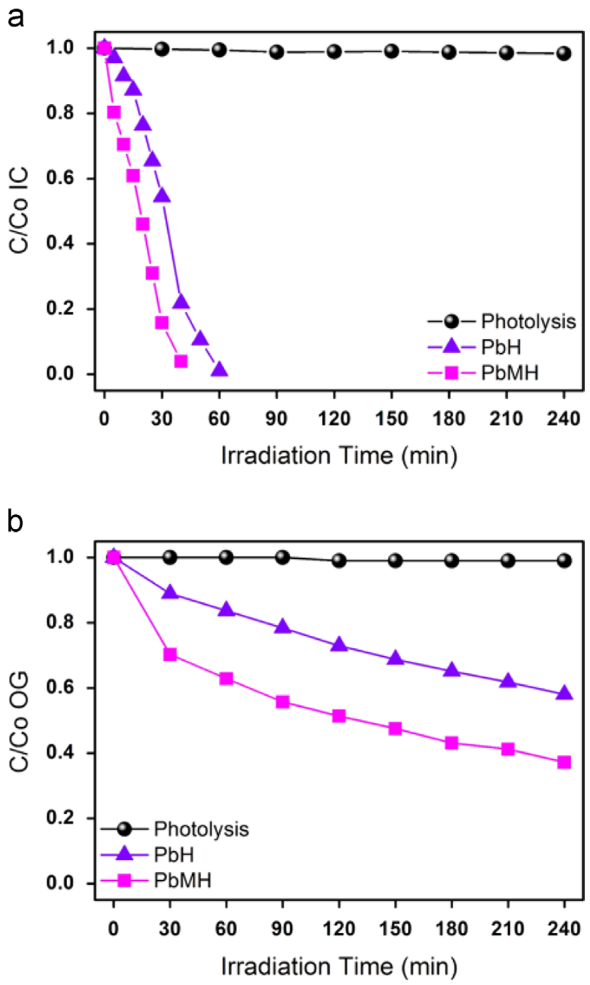

Fig. 4. Photodegradation of indigo carmine (a) and orange G (b) under UV–vis light irradiation for $PbMoO_4$ synthesized by the microwave-assisted solvothermal and solvothermal method.

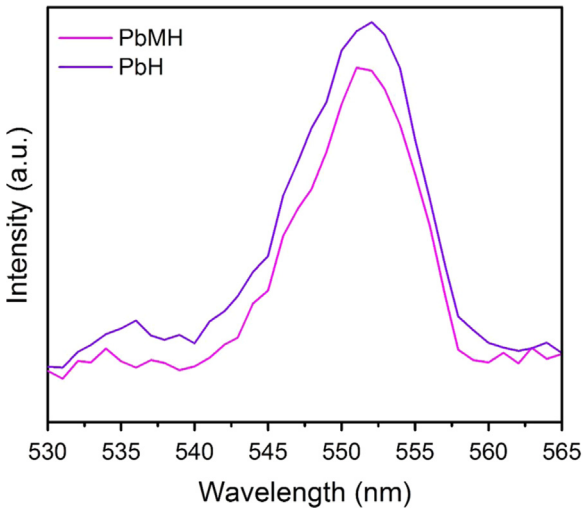

Fig. 5. Photoluminescence (PL) spectra of $PbMoO_4$ excited with a 350 nm wavelength.

near to 40% of OG was photodegraded by using the PbH photocatalyst. In the photocatalytic dye degradation, indigoid family (IC) is more degradable than azo dye family (OG) owing the ease of decarboxylation of a monocarboxylic acid, compared to the recalcitrant compounds obtained in the azo dyes as intermediates [28].

In order to determine the photocatalytic activity of PbMH and PbH in pharmaceutical compounds, the degradation of some organic compounds of this family was performed. The photocatalytic activity of PbH and PbMH samples was evaluated in the degradation of TC under UV–vis light irradiation, as is shown in Fig. 6(a). After photocatalytic reaction for 120 min, the highest TC degradation ratio was about 99% with a half-time of $t^1/_2 = 6$ min using PbMH sample as photocatalyst. It can be seen the PbH sample shows a lower photocatalytic activity with a $t^1/_2 = 80$ min. The increment in the difference of the half-times in antibiotic in comparison with the values observed for organic dyes could be attributed to the presence of oxamic acid produced from different ways to break some of the weakest bonds in the organic molecules by •OH radical, as is reported in the literature [29,30].

Fig. 6(b) shows the experiments of CIP photodegradation, belongs to the fluoroquinolones family, which is a new class of antibiotic. However, the PbMH sample showed a degradation of almost 100% of the antibiotic with a half-time of 7 min, which is 11 times minor than the obtained for PbH sample. During the CIP degradation, the hydroxylation intermediates were generated owing

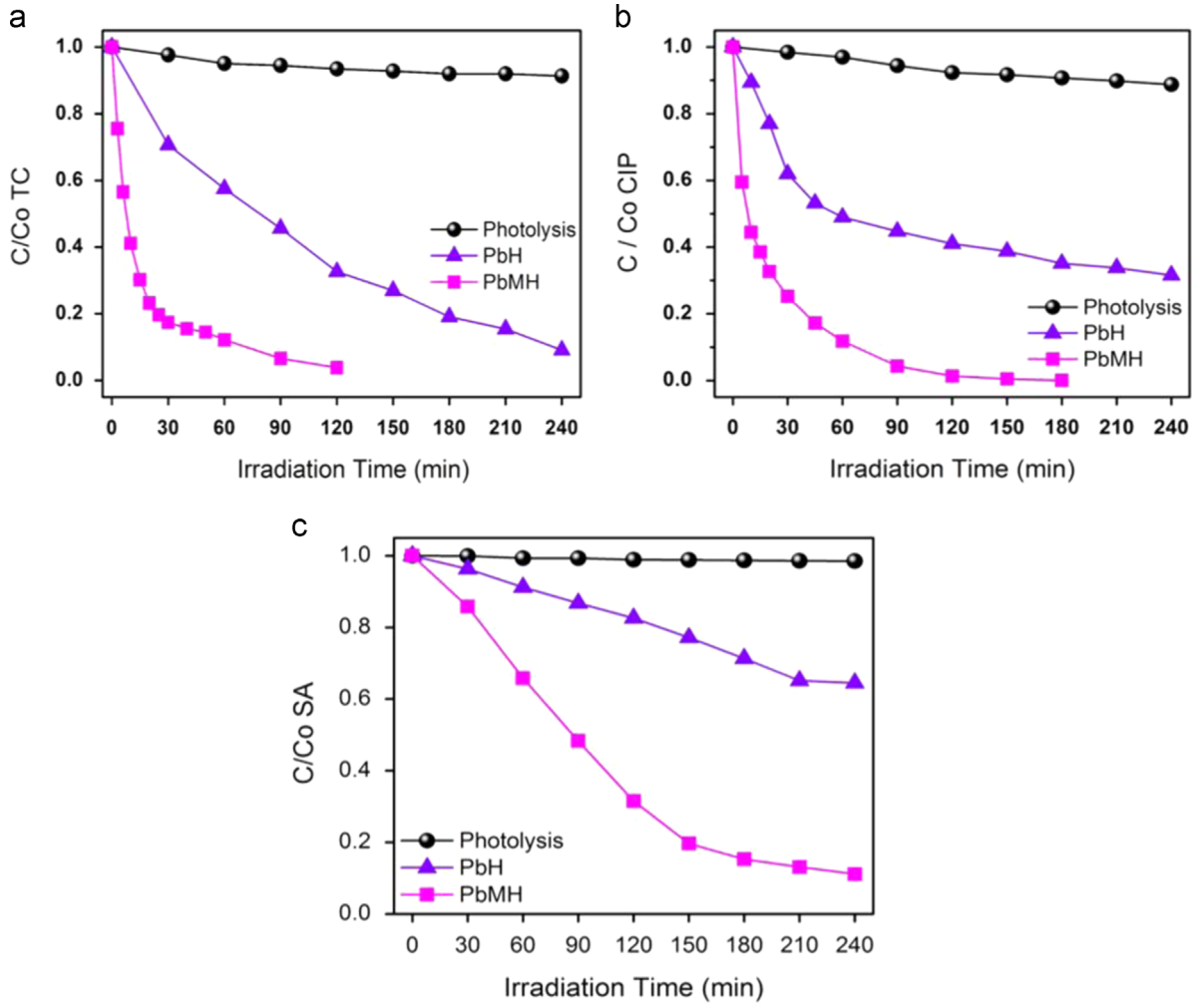

Fig. 6. Photodegradation of tetracycline (a), ciprofloxacin (b) and salicylic acid (c) under UV–vis light irradiation for $PbMoO_4$ synthesized by the microwave-assisted solvothermal and solvothermal method.

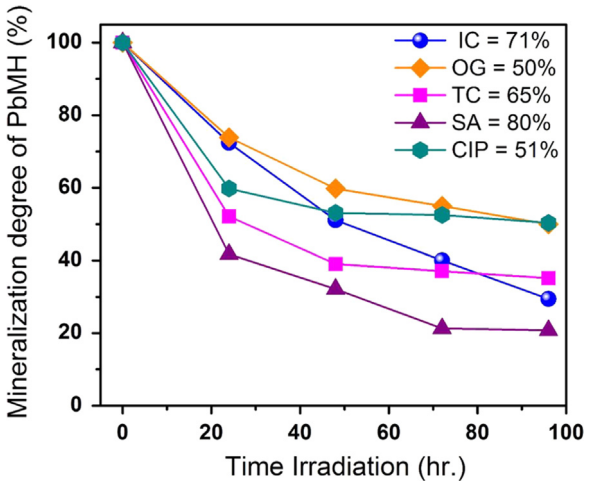

Fig. 7. Variation of the TOC during the mineralization of IC, OG, TC, SA and CIP under UV–vis light irradiation.

to breakdown of the piperazynilic ring from the CIP molecule after the oxidative and reductive processes. [31,32].

Salicylic acid (SA) photocatalytic degradation for PbMH and PbH under UV–vis light irradiation is illustrated in Fig. 6(c). The experiments were performed to examine the catalyst efficiency in the degradation process with a half-time of 75 and 312 min. So the PbMH powders exhibited the higher photocatalytic activity in the SA degradation under simulated sunlight irradiation, but the half-time was increasing in comparison with the others antibiotics, which could be attributed to the aromatic recalcitrant intermediates and carboxylic acids generated during the degradation of salicylic acid [33]. The photocatalytic behavior of the PbMH sample on the pharmaceutical compounds increases in the order: SA < CIP < TC which is influenced by the molecules generated during the process.

The total organic carbon (TOC) was measured in order to determine the mineralization efficiency of $PbMoO_4$, as is shown in Fig. 7. PbMH was selected as catalyst in TOC experiments due to the sample with the highest photocatalytic activity. The mineralization degrees were 71% for IC, 50% for OG, 65% for TC, 51% for CIP and 80% for SA after 96 h under UV–vis light irradiation, indicating a high mineralization degree of the pollutants. TOC content in the antibiotic mineralization experiments shows a quick reduction during the first 48 h of irradiation. Afterwards, the TOC content tends to have a semi-constant value, which could be attributed to the

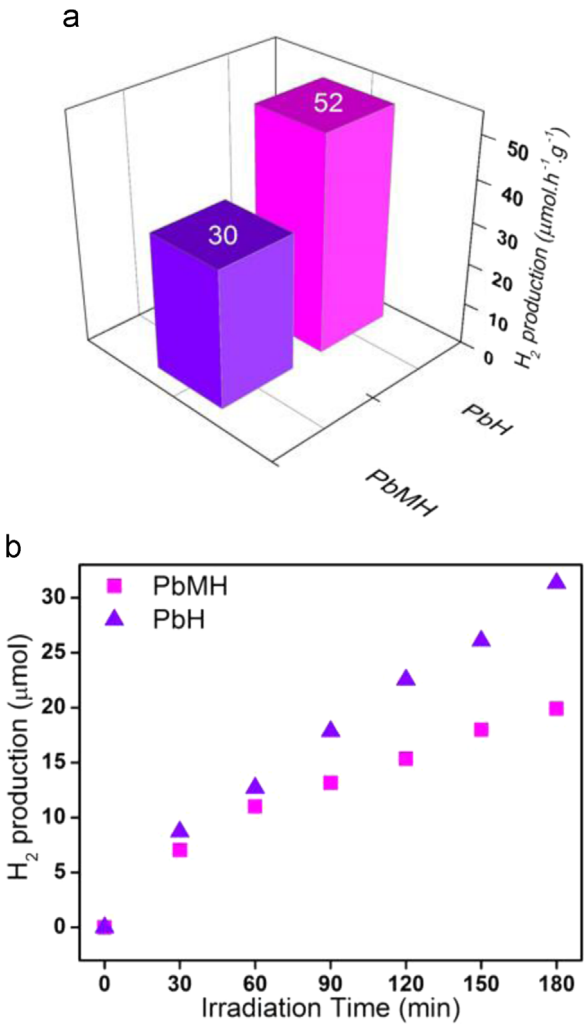

Fig. 8. Histogram showing the average H_2 production rate (a) and photocatalytic H_2 evolution (b) under UV light irradiation for $PbMoO_4$ as catalyst synthesized by the microwave-assisted solvothermal and solvothermal method.

formation of oxalic acid (the last by-product), which is hardly destroyed by radical •OH causing the mineralization time was increasing [29,33]. Otherwise, TOC content in the dyes was gradually decreasing with the reaction time increment.

3.3. Water splitting experiments

H_2 production under UV light irradiation was carried out using $PbMoO_4$ obtained by the microwave-assisted solvothermal (PbMH) and solvothermal (PbH) method. The PbH sample shows a H_2 production rate of 52 μmol h^{-1} g^{-1}, which is almost twice higher than the PbMH sample (30 μmol h^{-1} g^{-1}), as is seen in Fig. 8(a). Moreover, the PbH and PbMH samples exhibited a constant hydrogen production during 180 min of the reaction, as is seen in Fig. 8(b). The crystallinity degree is the main factor to enhance the photocatalytic activity for H_2 production [25]. Therefore, the highest photoactivity of PbH sample could be associated mainly with the crystallinity degree compared to the PbMH sample, as was revealed by XRD analysis (Fig. 1). High crystallinity degree decreased the defect concentration on the crystalline structure of the catalyst. These defects could act as recombination sites of the electron–hole pairs formed during the excitation of the oxide by the UV light irradiation.

4. Conclusions

$PbMoO_4$ samples were successfully synthesized with a high crystallinity degree and small average particle size obtained by the microwave-assisted solvothermal and solvothermal method. The photodegradation of indigo carmine, orange G, tetracycline, ciprofloxacin and salicylic acid was successfully evaluated using $PbMoO_4$ as catalyst under UV–vis illumination. These results indicate that PbH material has lower photocatalytic activity than PbMH material due to the particle size as main property that influenced the photoactivity in pollutants degradation in aqueous medium. On other hand, high crystallinity is the factor that influenced in the higher hydrogen generation for PbH sample. It is evidence that the $PbMoO_4$ as photocatalyst is a good candidate as the pollutant degradation and hydrogen production.

Acknowledgments

We wish to thank to the Universidad Autónoma de Nuevo León (UANL) for the financial support to the Project PAICYT 2015, the PRODEP Project: DSA/103.5/15/6797 and CONACYT for supports the Project no. 220792.

References

[1] L.M. Pastrana-Martínez, J.L. Faria, J.M. Doña-Rodríguez, C. Fernández-Rodríguez, A.M.T. Silva, Degradation of diphenhydramine pharmaceutical in aqueous solutions by using two highly active TiO_2 photocatalysts: operating parameters and photocatalytic mechanism, Appl. Catal. B 113–114 (2012) 221–227.

[2] Yan Yan, Shaofang Sun, Yang Song, Xu Yan, Weisheng Guan, Xinlin Liu, Weidong Shi, Microwave-assisted in situ synthesis of reduced graphene oxide-$BiVO_4$ composite photocatalysts and their enhanced photocatalytic performance for the degradation of ciprofloxacin, J. Hazard. Mater. 250–251 (2013) 106–114.

[3] Xiangdong Zhu, Yujun Wang, Dongmei Zhou, TiO2 photocatalytic degradation of tetracycline as affected by a series of environmental factors J. Soils Sediments 14 (2014) 1350–1358.

[4] Matthew Essandoh, Bidhya Kunwar, Charles U. Pittman Jr., Dinesh Mohan, Todd Mlsna, Sorptive removal of salicylic acid and ibuprofen from aqueous solutions using pine wood fast pyrolysis biochar, Chem. Eng. J. 265 (2015) 219–227.

[5] Danielle M. Schultz, Tehshik P. Yoon, Solar synthesis: prospects in visible light photocatalysis, Science 28–343 (2014) 6174.

[6] Wei Zhao, Yang Guo, Yasir Faiz, Wen-Ting Yuan, et al., Facile in-suit synthesis of $Ag/AgVO_3$ one-dimensional hybrid nanoribbons with enhanced performance of plasmonic visible-light photocatalysis, Appl Catal. B 163 (2015) 288–297.

[7] Wei Wang, Moses O. Tadé, Zongping Shao, Research progress of perovskite materials in photocatalysis and photovoltaics related energy conversion and environmental treatment, Chem. Soc. Rev. 44 (2015) 5371–5408.

[8] John Anthony Byrne, Patrick Stuart Morris Dunlop, John Hamilton Jeremy William, et al., A review of heterogeneous photocatalysis for water and surface disinfection, Molecules 20 (4) (2015) 5574–5615.

[9] Jillian M. Buriak, Prashant V. Kamat, Kirk S. Schanze, Best practices for reporting on heterogeneous photocatalysis, Appl. Mater. Interfaces 6 (15) (2014) 11815–11816.
[10] Ali Ayati, Ali Ahmadpour, Fatemeh F. Bamoharram, et al., A review on catalytic applications of Au/TiO_2 nanoparticles in the removal of water pollutant, Chemosphere 107 (7) (2014) 163–174.
[11] Diana B. Hernandez-Uresti, D. Sánchez-Martínez, A. Martínez-delaCruz, S. Sepúlveda-Guzmán, Leticia M. Torres-Martínez, Characterization and photocatalytic properties of hexagonaland monoclinic WO_3 prepared via microwave-assisted hydrothermal synthesis, Ceram. Int. 40 (2014) 4767–4775.
[12] Yijie Wu, Dongmei Chu, Ping Yang, Yukou Du, Cheng Lu, Ternary mesoporous WO_3/Mn_3O_4/N-doped graphene nanocomposite for enhanced photocatalysis under visible light irradiation, Catal. Sci. Technol. 5 (2015) 3375–3382.
[13] D. Papoulis., E. Kordouli., P. Lampropoulou, Rapsomanikis, et al., Synthesis, characterization and photocatalytic activities of fly ash-TiO_2 nanocomposites for the mineralization of azo dyes in water, J. Surf. Interfaces Mater. 2 (4) (2014) 261–266.
[14] T. Fotiou, T.M. Triantis, T. Kaloudis, A. Hiski, Evaluation of the photocatalytic activity of TiO_2 based catalysts for the degradation and mineralization of cyanobacterial toxins and water off-odor compounds under UV-A, solar and visible light, Chem. Eng. J. 261 (2015) 17–26.
[15] F.E. Osterloh, B.A. Parkinson, Recent developments in solar water-splitting photocatalysis, Mater. Res. Soc. Bull. 36 (2011) 17–22.
[16] X.B. Chen, S.H. Shen, L.J. Guo, S.S. Mao, Semiconductor-based photocatalytic hydrogen generation, Chem. Rev. 110 (2010) 6503–6570.
[17] A. Kudo, Y. Miseki, Heterogeneous photocatalyst materials for water splitting, Chem. Soc. Rev. 38 (2009) 253–278.
[18] H. Tong, S. Ouyang, Y. Bi, N. Umezawa, M. Oshikiri, J. Ye, Nano-photocatalytic materials: possibilities and challenges, Adv. Mater. 24 (2012) 229–251.
[19] J. Méndez-Ramos, J.C. Ruiz-Morales, P. Acosta-Moraa, J. del-Castilloc, A.C. Yanes, Rare-earth doped nano-glass-ceramics for extending spectral response of water-splitting semiconductor electrodes by high intense UV-blue up-conversion: turning the sun into blue, J. Power Sources 238 (2013) 313–317.
[20] T. Ikeda, A. Xiong, T. Yoshinaga, K. Maeda, K. Domen, T. Teranishi, Polyol synthesis of size-controlled Rh nanoparticles and their application to photocatalytic overall water splitting under visible light, J. Phys. Chem. C 117 (2013) 2467–2473.
[21] S. Obregón, A. Caballero, G. Colón, Hydrothermal synthesis of $BiVO_4$: structural and morphological influence on the photocatalytic activity, Appl. Catal. B: Environ. 117–118 (2012) 59–66.
[22] D.B. Hernández-Uresti, A. Martínez-de la Cruz, J.A. Aguilar-Garib, Photocatalytic activity of $PbMoO_4$ molybdate synthesized by microwave method, Catal. Today 212 (2013) 70–74.
[23] Eduardo de Moraes, Maurício Bomio, Valéria M. Longo, et al., Freezing distortions and photoluminescence property in $PbMoO_4$ micro-octahedrons: an experimental and theoretical study, Curr. Phys. Chem. 4 (1) (2014) 4–14.
[24] Chunxue Hao, Fusheng Wen, Jianyong Xiang, Photocatalytic performances of $BiFeO_3$ particles with the average size in nanometer, submicrometer, and micrometer, Mater. Res. Bull. 50 (2014) 369–373.
[25] Kai Yan, Guosheng Wu, Cody Jarvis, Jiali Wen, Aicheng Chen, Facile synthesis of porous microspheres composed of TiO_2 nanorods with high photocatalytic activity for hydrogen production, Appl. Catal. B: Environ. 148–149 (2014) 281–287.
[26] Sheng Chu, Ying Wang, Yong Guo, et al., Facile green synthesis of crystalline polyimide photocatalyst for hydrogen generation from water, J. Mater. Chem. 22 (2012) 15519–15521.
[27] A.M. Huerta-Flores, L.M. Torres-Martínez, D. Sánchez-Martínez, M. E. Zarazúa-Morín, $SrZrO_3$ powders: alternative synthesis, characterization and application as photocatalysts for hydrogen evolution from water splitting, Fuel 158 (2015) 66–71.
[28] R. Vinu, Giridhar Madras, Kinetics of sonophotocatalytic degradation of anionic dyes with nano-TiO_2, Environ. Sci. Technol. 43 (2) (2009) 473–479.
[29] C.I. Brinzila, N. Monteiro, M.J. Pacheco, et al., Degradation of tetracycline at a boron-doped diamond anode: influence of initial pH, applied current intensity and electrolyte, Environ. Sci. Pollut. Res. 21 (2014) 8457–8465.
[30] Joonseon Jeong, Weihua Song, William J. Cooper, et al., Degradation of tetracycline antibiotics: mechanisms and kinetic studies for advanced oxidation/reduction processes, Chemosphere 78 (2010) 533–540.
[31] Hai Taicheng An, Guiying Li Yang, et al., Kinetics and mechanism of advanced oxidation processes (AOPs) in degradation of ciprofloxacin in water, Appl. Catal. B: Environ. 94 (2010) 288–294.
[32] Tias Paul, Michael C. Dodd, Timothy J. Strathmann, Photolytic and photocatalytic decomposition of aqueous ciprofloxacin: transformation products and residual antibacterial activity, Water Res. 44 (2010) 3121–3132.
[33] Elena Guinea, Conchita Arias, Pere Lluis Cabot, et al., Mineralization of salicylic acid in acidic aqueous medium by electrochemical advanced oxidation processes using platinum and boron-doped diamond as anode and cathodically generated hydrogen peroxide, Water Res. 42 (2008) 499–511.